2021-01-0720 Published 06 Apr 2021

Evaluation of 48V and High Voltage Parallel Hybrid Diesel Powertrain Architectures for Class 6-7 Medium Heavy-Duty Vehicles

Mufaddel Dahodwala, Satyum Joshi, FNU Dhanraj, Nitisha Ahuja, Erik Koehler, Michael Franke, and Dean Tomazic FEV North America Inc.

Citation: Dahodwala, M., Joshi, S., Dhanraj, F., Ahuja, N. et al., "Evaluation of 48V and High Voltage Parallel Hybrid Diesel Powertrain Architectures for Class 6-7 Medium Heavy-Duty Vehicles," SAE Technical Paper 2021-01-0720, 2021, doi:10.4271/2021-01-0720.

Abstract

Electrification of heavy-duty trucks has received significant attention in the past year as a result of future regulations in some states. For example, California will require a certain percentage of tractor trailers, delivery trucks and vans sold to be zero emission by 2035. However, the relatively low energy density of batteries in comparison to diesel fuel, as well as the operating profiles of heavy-duty trucks, make the application of electrified powertrain in these applications more challenging. Heavy-duty vehicles can be broadly classified into two main categories; long-haul tractors and vocational vehicles. Long-haul tractors offer limited benefit from electrification due to the majority of operation occurring at constant cruise speeds, long range requirements and the high efficiency provided by the diesel engine. However, vocational applications can realize a significant benefit from electrified powertrains due to their lower vehicle speeds, frequent start-stop driving and shorter operating range requirements.

As the heavy-duty industry deals with solving challenges around the application of electrified powertrains, there are multiple pathways that can be explored to meet future regulatory requirements. This paper is the first part of a two-paper series that focuses on evaluating electrified solutions for Class 6-7 medium heavy-duty vehicles in the 2027 and beyond time frame. In this paper the focus is on investigation of near-term hybrid solutions that provide reasonable fuel efficiency improvements within a two-year payback period.

To investigate the various hybrid electric architectures, FEV has developed a system level approach for the selection and sizing of heavy-duty diesel hybrid powertrain components using GT-SUITE. The approach has been applied for a Class 6-7 urban vocational truck, which typically experiences low speed driving with frequent start-stops. A dynamic model for the baseline diesel vehicle was developed and calibrated to test data. The baseline diesel vehicle was then updated with hybrid powertrain components to evaluate different parallel hybrid architectures (P1, P2, P3, P4) at two different voltage levels: ≤48V (mild hybrid) and >150V (full hybrids). The evaluation was conducted over multiple drive cycles, including the ARB Transient Cycle and a real-world drive cycle. In the evaluation, key trade-offs were identified between fuel consumption, initial investment cost, payback period and freight efficiency. The trade-off analysis demonstrated that for a two-year payback period, a P3 architecture provided the best fuel consumption value for full hybrid applications. In a P2 or P3 configuration, a 48V system also showed considerable fuel efficiency improvements compared to the baseline diesel vehicle. The final P3 hybrid powertrain configuration for Class 6-7 vocational truck shows a 27% fuel consumption reduction for a 350V system while a 48V system shows a 22% fuel consumption reduction when considering a payback period of two years.

Introduction

As the transportation sector is continuously growing it is expected that the truck freight will continue to rise in the United States (US) by at least 1% every year for the next 25 years [1]. Class 3-8 medium to heavy-duty trucks, primarily used for on-road freight transportation, are responsible for 23% of the total transportation related Greenhouse Gas Emissions (GHG) in the US [1]. In Europe, heavy-duty vehicles are responsible for 5% of the total greenhouse gas emissions [1,2]. Reduction of GHG emissions from the transportation sector will have a major impact and has been undertaken by multiple US government agencies including the Environmental Protection Agency (EPA) and California Air Resource Board (ARB). EPA has already implemented Phase II GHG emission standards requiring 22-25% reduction in CO_2 emissions by 2027 [3]. The European Union [EU] has also mandated that certain categories of heavy-duty trucks reduce their CO_2 emissions by 30% of 2019 emission levels in 2030 [4]. ARB's Advanced Clean Truck regulation released in June 2020 also mandates that the truck Original Equipment Manufacturers (OEM's) begin selling a larger share of Zero/Near-Zero Emission Vehicles (ZEV/NZEV) in

California from 2024 [5]. The regulation requires that by 2035, 75% of all the Class 4-8 non-tractors and 40% of all Class 7-8 tractors sold by the OEM's in California should be ZEV's and/or NZEV's [5].

The legislations are aimed toward accelerating the adoption of electrified powertrain solutions such as Battery Electric Vehicles (BEVs) and Fuel Cell Vehicle (FCVs) for future applications. However, at present, due to the higher cost of electrified powertrain architectures when compared to diesel applications, it is expected that the transportation industry will remain in a transition period between 2020 and 2040. This transition period, also referred to as the 'messy middle' by the North American Council for Freight Efficiency (NACFE) in its latest guidance report, suggests of a time period where the truck industry will be flooded with multiple fuel choices, infrastructure development initiatives, learning, and innovations [6, 7, 8].

During this transition period truck OEM's are expected to apply an increased level of electrification based on cost effectiveness, market readiness, maturity, ease of integration and operability [9]. The level of electrification for medium to heavy-duty trucks will vary based on their application. For example, a Class 8 long-haul truck which operates at cruising speed for most of its drive cycle could benefit from a 48V mild hybrid configuration and accessory electrification. Class 3-7 vocational trucks which operate at relatively low speeds and experience frequent start-stops can achieve a 15-25% fuel efficiency improvement from the application of a mild or full hybrid system [10,11,12,13]. Class 3-7 vocational applications are also suitable candidates for battery and fuel cell electric powertrains and range extenders. The general trend and guidelines for electrification on passenger cars/light trucks may not be valid for Class 3-7 urban vocational vehicles as the segment faces specific challenges including; lower production volumes, lost payload, durability requirements, varying packaging constraints, varying operating vehicle weight, long vehicle useful life, wide range of operating drive cycles, and engine exhaust gas aftertreatment performance requirements [10]. A comprehensive evaluation of various electrification technologies for the heavy-duty segment in terms of their suitability to meet a wide range of applications and representative drive cycles, impact on cost of ownership and potential CO_2 benefits is certainly required.

In this first part of a two-paper series, four different parallel hybrid architectures for Class 6-7 vocational applications were analyzed at two different voltages levels: 48V mild hybrid and full hybrid (>150V). The second part of this two-paper series explores a variety of range extender powertrains along with battery electric and fuel cell electric vehicles for Class 6-7 vocational applications. The baseline vehicle model for the Class 6-7 vocational truck was developed using GT-SUITE. After correlating the baseline vehicle model to experimental data, the model was updated with hybrid components to evaluate multiple parallel hybrid configurations. The performance of different hybrid layouts with 48V mild hybrid and full hybrid systems were evaluated on the ARB Transient and real-world drive cycles. Performance of the different parallel hybrid configurations was compared based on CO_2 emissions, fuel consumption, payback period, cost of ownership and freight efficiency.

Vehicle Model Development and Validation

A dynamic one-dimensional vehicle model of a Freightliner M2 106 vehicle was developed in GT-SUITE [14] for this analysis. The vehicle specifications and key modeling parameters are described in Table 1. A model based approach was implemented for this investigation to allow for evaluation of various hybrid architectures with maximum flexibility and acceptable computation time [15]. Figure 1 shows the layout of the baseline vehicle model developed in GT-SUITE. A map-based engine model was developed with specific fuel consumption and torque output as a function of engine speed and throttle position. Figure 2 provides the specific fuel consumption map of the engine.

TABLE 1 Vehicle specifications and key modeling parameters for longitudinal vehicle dynamics [14].

Vehicle Model	Freightliner M2 106
Chassis Type	132" BBC Extended Cab
Vehicle Curb Mass	15,695 lb
Total Loaded Vehicle Mass	25,000 lb
Engine Type	Cummins ISB 6.7L
Engine Displacement	6.7 L
Bore x Stroke	107 mm×124 mm
Advertised Rated Power	300 hp @ 2,600 rpm
Maximum Engine Torque	650 lb-ft @ 1,600 rpm
Transmission Type	Allison 2000 Series 6-Speed
Final Drive Ratio	5.5
Axle Configuration	4×2
Tire Rating	11R22.5
Tire Rolling Radius	0.525 m
Rolling Resistance Coefficient	0.009
Vehicle Frontal Area	10.1 m^2
Aerodynamic Drag Coefficient	0.6
Auxiliary Electrical Load	2 kW

FIGURE 1 1D model layout in GT-SUITE for baseline M2 106 vehicle [14].

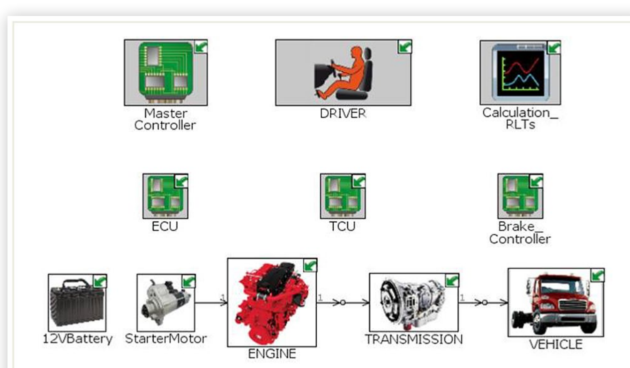

FIGURE 2 Brake specific fuel consumption (BSFC) map for Cummins ISB 6.7L engine [14].

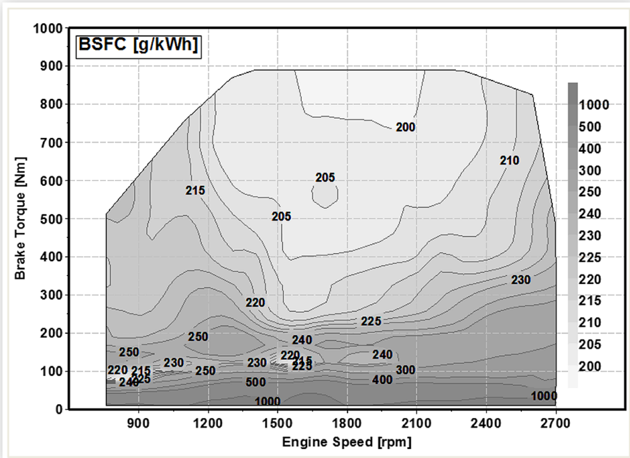

FIGURE 3 Baseline vehicle model validation on custom drive cycle (experimental fuel economy - 4.15mpg, simulation fuel economy - 4.20 mpg) [14].

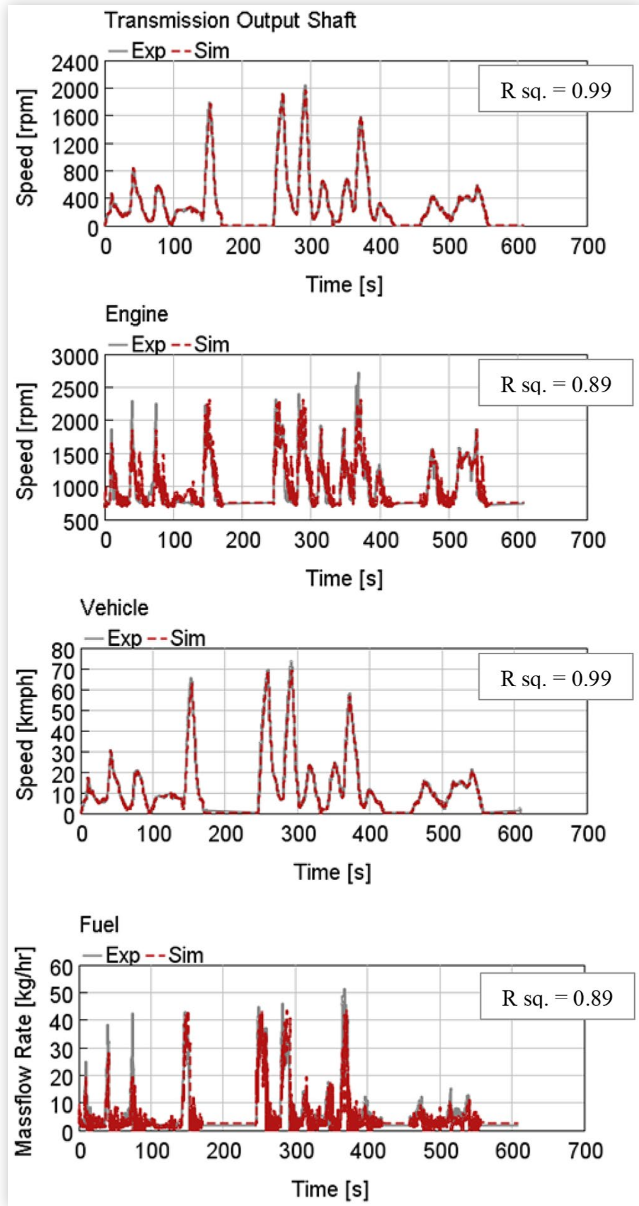

The transmission was modeled as a lumped inertia component. The torque converter was modeled by specifying performance curves of input capacity factor and torque ratio versus speed ratio. Additional details regarding the baseline model development can be referenced from a previously published study [14].

Other driveline components, such as, axles, tires and differential, were modeled by specifying component inertias and power transfer efficiency. Friction brakes were modeled and sized to ensure that the required deceleration was achieved to follow different vehicle drive cycle profiles. A 12V battery and starter motor were also included in the model to account for auxiliary electrical load and engine startup losses. The baseline model was correlated to test data collected on a real-world drive cycle as shown in Figure 3. The average fuel consumption was correlated within 2% of the measured data.

Hybrid Powertrain Integration

After the baseline model was correlated, four different parallel hybrid architectures were evaluated for a Class 6-7 vocational application as shown in Figure 4. All four parallel hybrid powertrains were evaluated at two voltages levels: 48V mild hybrid and full hybrid (>150V). The baseline vehicle model was integrated with a motor-generator, gear box, power electronics, lithium-ion Nickel Manganese Cobalt Oxide (NMC) battery, battery management system, engine clutch and a supervisory control strategy. An optional engine starter motor was implemented based on the maximum motor-generator torque whereas a DC-DC converter replaced the lead-acid battery from the conventional vehicle model.

For the P1 parallel hybrid architecture, the engine was directly connected to a motor-generator unit which was then connected to the transmission through the torque converter and a lockup clutch assembly. The motor-generator unit acted as an engine starter along with providing additional torque during acceleration to assist the engine and perform load shifts. During vehicle deceleration the motor-generator unit also acted as generator for energy recuperation. In the P2 parallel hybrid architecture an additional clutch and a motor-generator unit were introduced between the engine and the transmission. The clutch was connected to the engine and motor-generator was connected to the transmission through the torque converter and a lockup clutch assembly. The introduction of the clutch between the engine and the motor-generator allowed the engine to shut down during deceleration and improved energy recuperation compared to the P1 parallel hybrid architecture. The P3 parallel hybrid architecture was developed by connecting the motor-generator unit to the transmission output shaft with a clutch. A starter motor was applied for engine starting. The P3 parallel hybrid architecture

FIGURE 4 Parallel hybrid powertrains evaluated in the study.

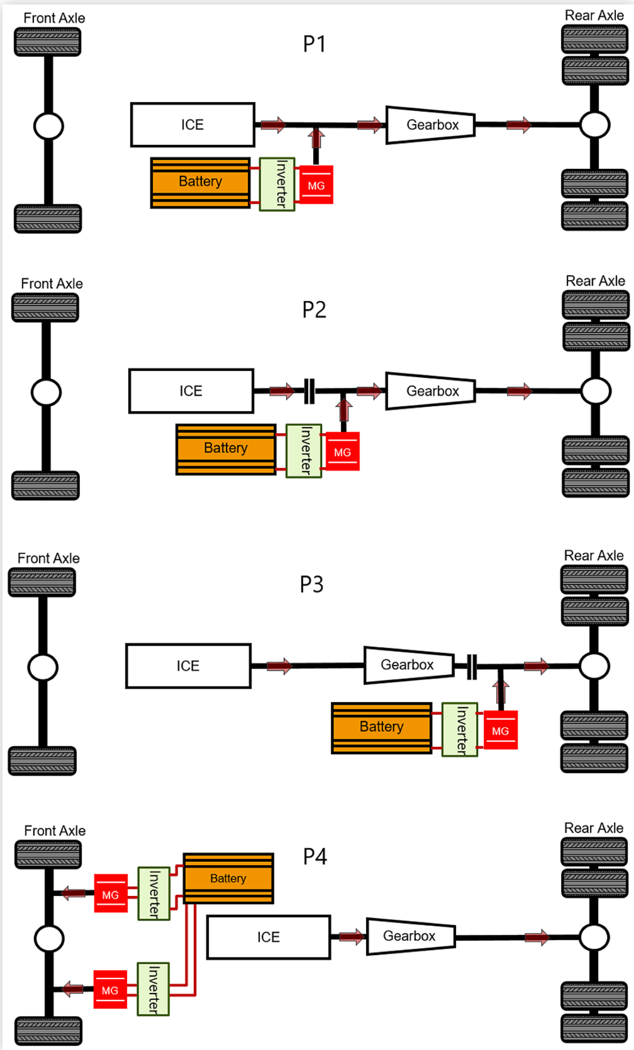

provided the opportunity for highest energy recuperation as the driveline could be disconnected during deceleration and braking events. Finally, in the P4 parallel hybrid architecture two motor-generators were directly coupled to the front axle of the vehicle. Here again, a starter motor was included for engine starting. The P4 architecture allowed for a four-wheel drive capability. Figure 5 shows a schematic of the modified GT-SUITE model with the motor-generator unit connected at different locations depending upon the parallel hybrid architecture under consideration.

Axial type permanent magnet BLDC (Brushless Direct Current) technology was selected for the motor-generator due to its high efficiency, higher torque output and packaging advantage [16]. A map-based motor-generator model was developed with specified maximum and minimum torque curves and combined motor-inverter efficiency as shown in Figure 6. For additional details on the map-based generator please refer to the previous study [14]. Maximum motor-generator torque during charge (1C) and discharge (3C) operation were also limited by battery capacity. Figure 7 shows the specified efficiency map for a BLDC motor-generator measured

FIGURE 5 Vehicle model layout in GT-SUITE for parallel hybrid powertrain configurations.

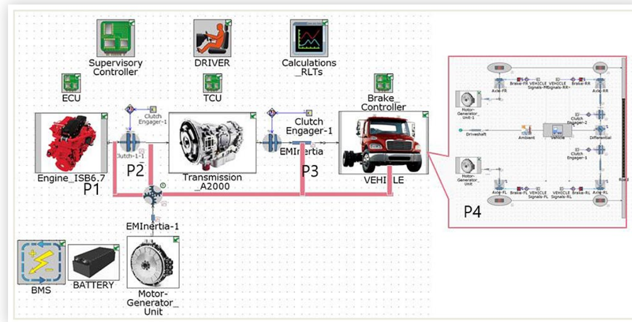

FIGURE 6 Parameterized motor-generator maximum/minimum torque curves [14].

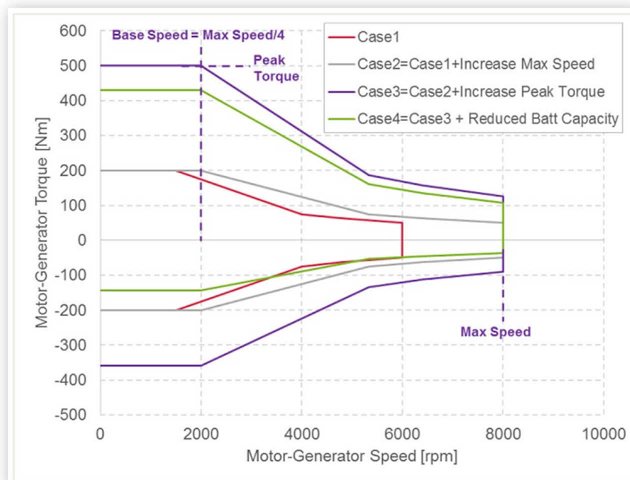

at 250V with a maximum speed of 8,000 rpm. Efficiency values for the motor maps were scaled using global factors based on operating voltage and motor-generator maximum speed. The scaling factors were derived from measured data from different axial BLDC motor-generators operated at different voltage levels and maximum speeds [14]. Table 2 compares the

FIGURE 7 250V motor-generator efficiency map specified in the motor-generator model [14].

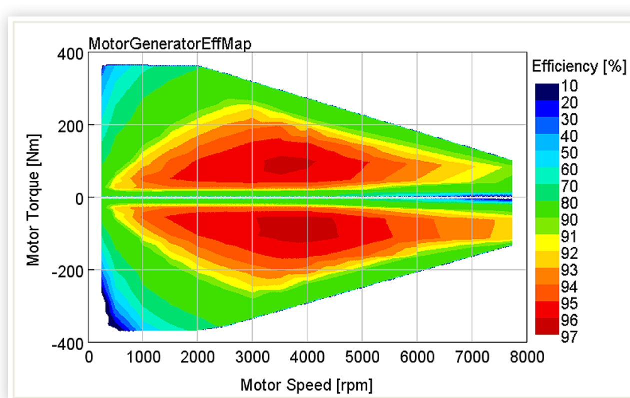

TABLE 2 Specifications of the 48V and full hybrid motor-generator map used in the study.

	250V Electric Motor	48V Electric Motor
Motor Rated Power	78 kW	7.85 kW
Maximum Speed	8,000 rpm	12,000 rpm
Maximum Torque	370 Nm	50 Nm

TABLE 3 Battery cell specifications for the GT-SUITE model [14].

Cell Specification	Value
Formulation	Li-Ion NMC 18650
Nominal Capacity	2.05 Ah
Maximum Charge Rate	1C
Maximum Discharge Rate	3C
Nominal Temperature	300K
Nominal Cell Voltage	3.8 V
Maximum Cell Voltage	4.2 V
Minimum Cell Voltage	2.75 V

baseline motor specification used for the 48V mild and full hybrid investigations.

The NMC battery technology was chosen for this application due to its higher specific capacity. A Thevenin electrical-equivalent circuit-based battery cell was modeled by specifying the open-circuit voltage, series internal resistance and RC branches to model the electrochemical dynamics. Battery cell State of Charge (SOC) was also modeled using the default approach available within GT-SUITE as shown in Equation 1.

$$SOC(t) = \frac{Capacity_{init} - \int_0^t I_{oc}dt}{Nominal\ Capacity} \quad (1)$$

Table 3 provides the parameters of the battery cell model as obtained from references [11,12,13]. Battery cells were arranged in series and parallel to vary battery voltage and capacity. Battery cooling and cell balancing were not considered in this study; however, a battery management system was introduced to restrict battery terminal voltage and current to their acceptable hardware limits. In addition, a cell aging model was implemented to predict battery capacity deterioration over time based on depth of discharge, average voltage and current [18,19].

A constrained on-off control strategy was selected for parallel hybrid powertrain management [20]. The control strategy determines the power split between engine and motor-generator based on the torque demand and battery SOC. A rule-based control strategy was selected over model-based optimization strategies such as, equivalent charge minimization strategy, dynamic programming, due to the computational limits of the engine control unit. The load regions and the corresponding torque divisions between the engine and the motor-generator map are shown in Figure 8. The lower torque curve, Tc, corresponds directly to the maximum torque curve of the motor-generator, while the torque curve, Tb, was setup as a function of the motor-generators maximum torque capacity. Topt and Ta indicate the minimum Brake Specific Fuel Consumption (BSFC) line and the maximum engine

FIGURE 8 Map-based control strategy used for optimization [14].

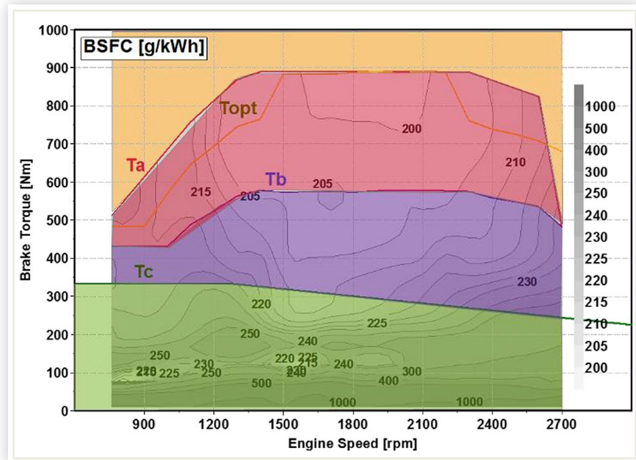

FIGURE 9 Control strategy performance on ARB transient cycle for the P2 hybrid architecture [14].

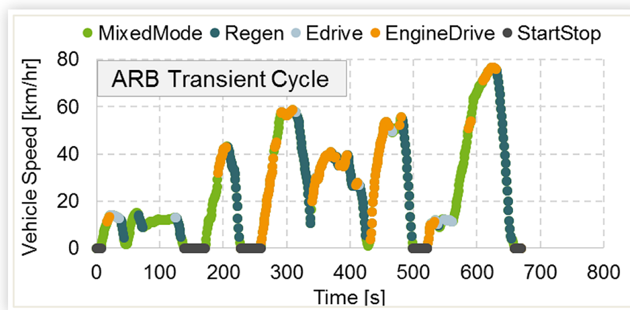

torque curve, respectively. Hysteresis loops were also implemented to prevent frequent engine start-stops between various control modes. Additional details on the applied control strategy can be referenced in the previous study [14].

Figure 9 shows the various operating modes of hybrid vehicle as enabled by the implemented control strategy on the ARB transient cycle for the P2 configuration. The ARB transient cycle allowed significant electric drive and energy recuperation opportunities due to its lower average vehicle speed and frequent start-stop. The mixed-mode indicates torque split operation between the engine and the motor-generator except during braking events at low vehicle speeds where mixed mode reflects engine idling. Battery SOC was sustained within 2% of the initial SOC at the end of the cycle.

In order to calculate the additional cost and weight with hybrid components, cost functions were implemented in the vehicle model as shown in Table 4. The cost function used for the hybrid components were estimated based on internal vehicle benchmark studies conducted on hybrid applications and published data in literature [21]. Additional calculations were added to the vehicle model to determine the fuel consumption, freight efficiency and payback period as shown in Table 5. As part of the analysis the cost of ownership at the eight-year mark was also evaluated. In order to compute the cost of ownership, the various cost function for the baseline

TABLE 4 Added cost and weight functions considered in the model for DoE optimization [14].

Parameter	Function
Battery Cost	$331/kWh
Motor Generator Cost	$7.9/kW
Power Electronics Cost	$9.9/kW
Battery Weight	12.8 kg/kWh
Motor-Generator + Power Electronics Weight	0.15 kg/kW

TABLE 5 Additional calculations used for optimization.

Fuel Consumption	$\dfrac{DGE\ Fuel[gal] + \dfrac{Battery\ Energy\ Change[kWh]}{Diesel\ Gal\ Equivalent[kWh/gal]}}{Total\ Miles\ Driven(mi) * Vehicle\ Weight[ton]}$
MPGe	$\dfrac{Total\ Miles\ Driven(mi)}{Fuel[gal] + \dfrac{Battery\ Energy\ Change[kWh]}{Diesel\ Gal\ Equivalent[kWh/gal]}}$
Freight Efficiency	$\dfrac{Total\ Miles\ Driven(mi) * Cargo\ Weight[ton]}{DGE\ Fuel[gal] + \dfrac{Battery\ Energy\ Change[kWh]}{Diesel\ Gal\ Equivalent[kWh/gal]}}$
Payback Period	$\dfrac{Added\ Powertrain\ Cost[\$] / Fuel\ Cost[\$/gal]}{\left(\dfrac{Annual\ Miles[mi/yr]}{Conv.MPGe[mi/gal]} - \dfrac{Annual\ Miles[mi/yr]}{Hybrid\ MPGe[mi/gal]}\right)}$

TABLE 6 Parameters used for cost of ownership calculations.

Vehicle Annual Mileage	24,000 miles
Cost of Ownership Time Period	~8 years or 192,000 miles
Base Vehicle Cost	$70,000
Total Additional Cost	Electrified Powertrain Cost - Conventional Powertrain Cost
Operation and Maintenance Cost [22]	Diesel $0.1375/mi HEV $0.2285/mi
Fuel Cost	Diesel $3.12/gal
Lost Payload Income [23, 24]	15.6 cents/ton-mile

vehicle, added electrified components, lost payload income and operation and maintenance cost were added to the model. The values used for this cost function are provided in Table 6.

Results and Discussion

After the map-based control strategy was validated, different hybrid configurations, as outlined earlier in the paper, were evaluated at two different voltage levels: 48V mild hybrid and full hybrid (>150V). The optimization for each configuration was carried out on the ARB transient cycle. A five variable DoE was conducted for each parallel hybrid configuration at two different voltage levels as shown in Table 7. The results were optimized using the FEV xCAL DoE tool [25] using the optimization criteria outlined in Table 8

TABLE 7 Parameters used for DoE study.

Parameters	Full Hybrid Range	Mild Hybrid Range
MG Peak Torque	50-500 Nm	20-180 Nm
MG Maximum Speed	2,000-20,000 rpm	2,000-20,000 rpm
Battery Voltage	150-760V	48V
Battery Capacity	20-100 Ah	10-100 Ah
Motor Gear Ratio	1-8	1-8

TABLE 8 Optimization criteria used in FEV×CAL DoE tool.

Optimization Qty	Optimization Objective	Weight
Fuel Consumption Reduction	Maximize	1.0
Freight Efficiency Improvement	Maximize	1.0
Total Added Weight	Minimize	0.1
Total Added Cost	Minimize	0.2
Total Battery Cells	Minimize	0.1
Battery Life	Maximize	0.1
Motor Torque	Minimize	0.1
Payback Period	Minimize	0.5

FIGURE 10 Tradeoff analysis of 48V mild and full hybrid configurations.

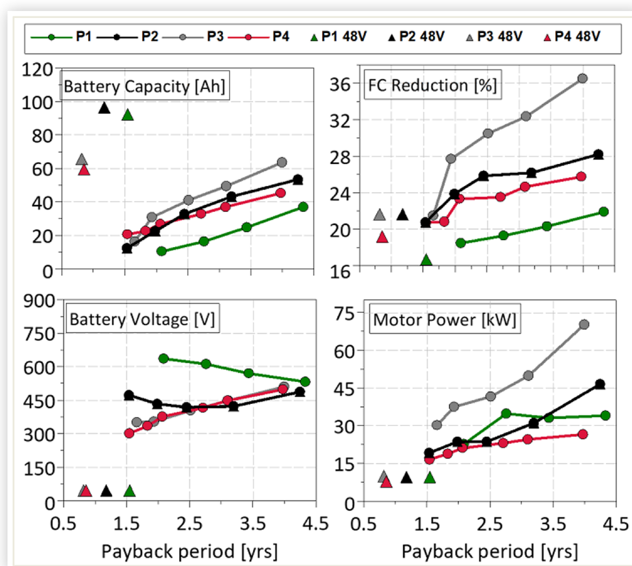

Figure 10 compares the fuel consumption reduction, battery capacity, battery voltage and motor power for the four different parallel hybrid architectures at two different voltage levels against the total payback period. For each configuration with the 48V mild hybrid system only one unique solution is presented, representing the maximum fuel consumption reduction within a two-year payback period. For the full hybrid configuration, multiple battery capacity, voltage and motor solutions are presented based on the different payback periods.

When comparing the various architectures at higher voltages (>150V), it is clear that the 350V P3 configuration provides the maximum fuel consumption (FC) benefit across the complete range of payback period considered. The higher FC reduction with the 350V P3 configuration is achieved due

FIGURE 11 Comparison of different parallel architectures based on added cost, weight and battery life.

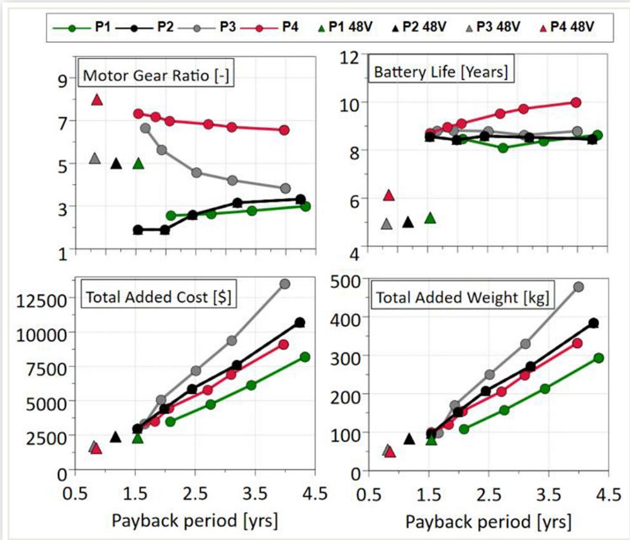

to the integration of the electric motor after the transmission. In the P3 configuration, the electric motor is able to achieve higher regeneration efficiency due to the elimination of the losses from the transmission and engine during regeneration when compared to the P1 and P2 configurations. The P4 configuration, which provides the maximum regeneration capability, shows limited FC reduction due to the relatively lower motor power applied. In the P4 configuration the maximum applied motor speed is limited due to the gear ratio limit of 8:1, which therefore limits the maximum power capability.

In the 48V configuration, the P2 and P3 configurations demonstrate a similar fuel consumption benefit. In both configurations (P2 and P3) the motor rated power is limited to 8.9 kW. If a motor with higher rated power is applied in the P3 configuration it results in improved FC reduction, but the two-year payback period criteria is not satisfied. Even though both 48V P2 and P3 configurations show similar fuel consumption benefit, the P3 solution is preferred due to the lower battery capacity and therefore a lower payback period of less than one year. Further comparison of the total added weight and cost for the two P3 configurations reveals that the 48V mild hybrid solutions result in a much lower initial investment of less than $2,000 compared to over $4,000 for the full hybrid. Another advantage of the 48V mild hybrid application is the lower payload penalty due to negligible increase in added weight as shown in Figure 11.

Figure 12 compares the CO_2 reduction and freight ton efficiency improvement for the four unique 48V configurations shown in Figure 10 along with all four full hybrid configurations with a two-year payback period. As shown in Figure 12, the highest CO_2 reduction of 24% is achieved with the P3 full hybrid configuration, however the P3 48V configuration also shows an 18% reduction in CO_2 emissions. When considering the Phase 2 GHG regulations for Class 6-7 urban vocational applications, as highlighted in Figure 13, a 48V P3 configuration is capable of achieving the CO_2 reduction targets. The freight ton efficiency improvements also show a

FIGURE 12 CO_2 improvement and freight ton efficiency improvement comparison.

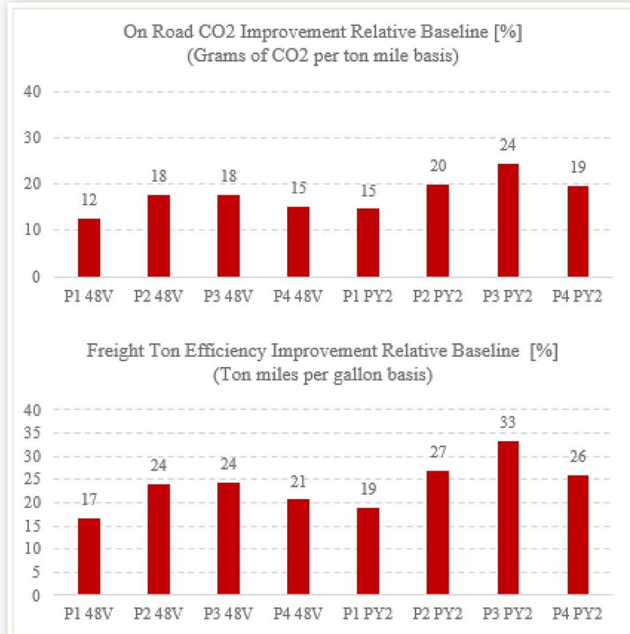

FIGURE 13 EPA 2027 phase-2 GHG regulations for Class 6-7 urban vocational applications.

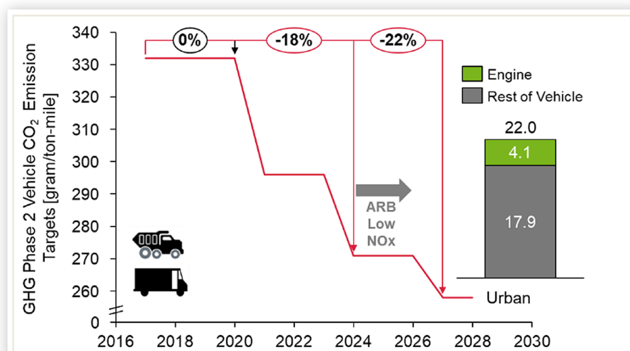

similar trend as the CO_2 reduction where the P3 full hybrid shows the largest improvement in freight ton efficiency for the full hybrid configurations.

Figure 14 compares the load shift on the engine operating map for the ARB transient cycle for two optimum P3 configurations: 48V and full hybrid with a two-year payback period. For the 48V P3 hybrid configuration with limited electric motor power capability, the hybrid controller is able to eliminate the engine operation at low to medium speed (700 - 1,500 rpm) and low loads (under 100 Nm). When applying a 350V P3 hybrid configuration, the 30kW electric motor is able to replace a larger area of the engine operation on the ARB Transient cycle, thereby resulting in a higher fuel consumption benefit and a CO_2 emission reduction. Referring again to Figure 12, as the payback period criteria is relaxed, the battery voltage increases and allows the application of higher power electric motors. The larger electric motor allows for a further

FIGURE 14 Load shift with P3 48V mild and full hybrid configurations on the baseline BSFC map.

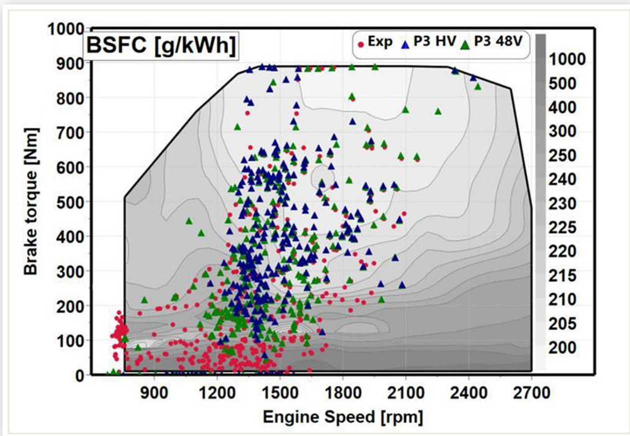

FIGURE 15 Motor operating points on a scaled map for the P3 350V hybrid.

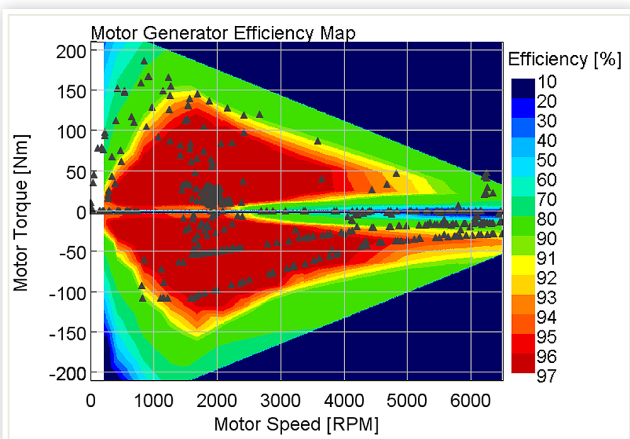

replacement of the engine operating point resulting in an increase in fuel consumption benefit.

The performance of the different hybrid configurations highlighted in Figure 10 were derived using motor maps that were scaled as per the procedure outlined in the hybrid powertrain integration section. Figure 15 shows the efficiency contours for a 350V electric motor that was scaled using the baseline motor maps provided in Figure 7. In order to validate the performance of the P3 hybrid configuration with a scaled motor map, the specifications for the scaled motor map were entered in the JMAG tool to derive a realistic motor map. Figure 16 shows a motor map that was obtained using the JMAG tool. The motor map obtained from the JMAG tool had a higher base speed and rated power when compared to the scaled maps used in our analysis. However, both maps show that the majority of the operating points are in an efficient region on the motor map. Table 9 outlines the fuel consumption reduction with the scaled map versus the JMAG map. The fuel consumption reduction predicted with the scaled maps were within 0.5% of the value predicted from the JMAG maps. This result confirms that the approach used for scaling the motor maps within this study were appropriate.

FIGURE 16 Motor operating points on JMAG motor map.

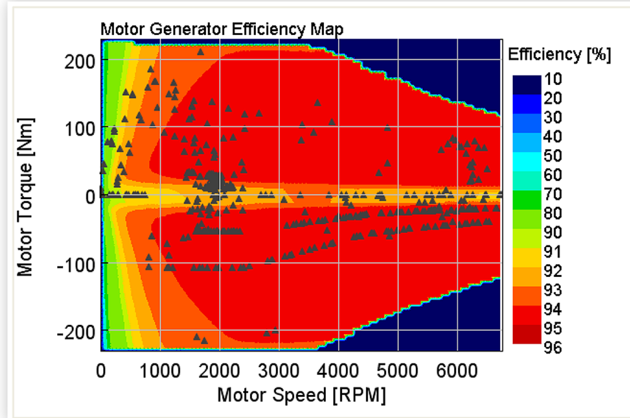

TABLE 9 Parameters of the scaled motor versus the JMAG motor maps.

Parameter	Scaled Maps	JMAG Maps
Motor Rated Power	38 kW	79 kW
Maximum Speed	6,700 rpm	6,700 rpm
Maximum Torque	213 Nm	213 Nm
FC Reduction	27.7%	28%

FIGURE 17 Energy loss comparison between P3 48V mild and full hybrid.

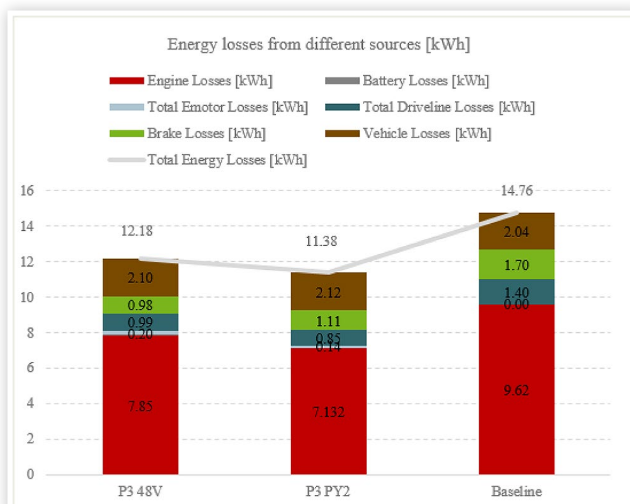

A further comparison of the 48V and full hybrid P3 configurations in terms of energy losses is highlighted in Figure 17. The P3 full hybrid configuration shows considerably lower engine losses due to the shift in engine operating profile as highlighted in Figure 14. The energy losses in the hybrid component and transmission are comparable between both configurations. Overall, for the P3 configuration, the full hybrid shows 0.8 kWh lower energy losses when compared to the 48V mild hybrid solution.

Figure 18 compares the cost of ownership between the two P3 configurations against the baseline diesel vehicle. The 48V P3 mild hybrid configuration shows the lowest cost of

FIGURE 18 Cost of ownership at eight years for P3 48V and full hybrid compared to baseline diesel vehicle.

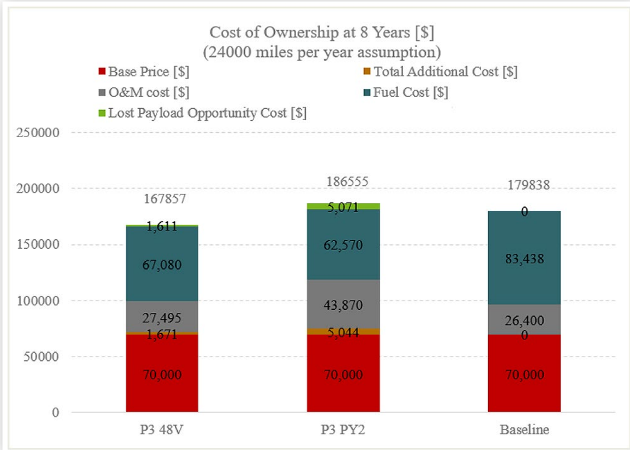

ownership at the 8-year mark. The 48V mild hybrid benefits from the lower operating and maintenance costs when compared to the full hybrid application while also performing significantly better in terms of the fuel cost when compared to the baseline diesel vehicle. The payload penalty with the 48V concept is also minimal due to a limited increase in weight. On the other hand, the P3 full hybrid has the highest cost of ownership mainly from the higher operating and maintenance costs, which are not offset sufficiently by the reduced fueling cost when compared to the 48V P3 mild hybrid configuration.

To this point, the analysis for the different hybrid architectures has been conducted on the ARB transient cycle which has relatively high weighting for determining the CO_2 emissions for vocational applications. However, the end user is concerned about fuel consumption improvements and subsequent return on investment on customer specific routes. In order to consider this impact, a custom drive cycle was develop using the GT-RealDrive feature as shown in Figure 19. The cycle was derived based on a typical operating profile experienced by a Class 6-7 delivery truck. The cycle considered included considerable low speed operation during city delivery with specific times of vehicle stop. Figure 20 compares the CO_2 reduction and freight efficiency improvement for both P3 configurations on real-world drive cycle. When compared to the ARB transient cycle, both P3 configurations show higher CO_2 reduction and freight efficiency improvements on the real-world drive cycle. For the P3 48V configuration, the CO_2 reduction improved by 2% for the real-world drive cycle

FIGURE 19 Real-world drive cycle generated from GT-power.

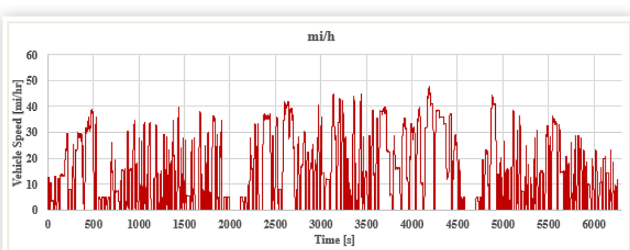

FIGURE 20 CO_2 reduction and freight ton efficiency improvement for P3 architectures compared on the ARB transient and real-world drive cycles.

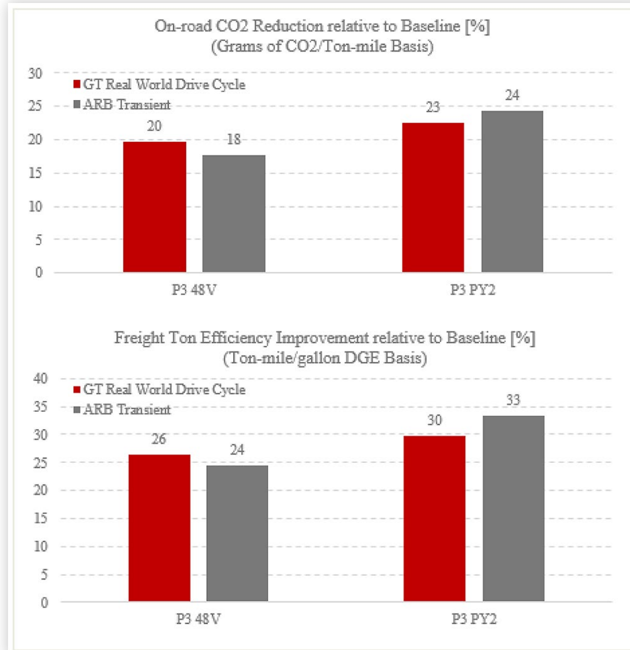

when compared to the ARB transient cycle. The higher CO_2 reduction also leads to improved freight ton efficiency. When compared on the real-world drive cycles, the difference in CO_2 improvement between the P3 mild hybrid and full hybrid application is 3% compared to the 6% difference when evaluated on the ARB transient cycle. These results further highlight the importance of considering both certification and real-world drive cycles when optimizing hybrid architecture/component specifications.

Conclusions and Future Work

In this paper key trade-offs were identified between fuel consumption, CO_2 reduction, freight ton efficiency, initial cost, payback period and vehicle weight for a Class 6-7 urban vocational parallel hybrid diesel powertrain vehicle. Four different hybrid configurations at two different voltage levels were considered for this analysis: 48V mild hybrid and full hybrid (>150V). The analysis was conducted using a dynamic vehicle model developed using GT-SUITE. The baseline diesel vehicle was calibrated against test data from real-world drive cycles. The performance maps of the baseline diesel engine were obtained from engine dynamometer testing. Once correlated, the baseline model was updated with hybrid powertrain components including, a battery model, an electric motor with a gear box and a battery management system. The vehicle model was analyzed with the hybrid components applied in four different approaches, resulting in P1, P2, P3 and P4 configurations.

The trade-off analysis demonstrated that when considering a two-year payback period, a 350V P3 architecture provided the greatest fuel consumption benefit at 27%. In a P3 configuration, the 48V mild hybrid system also showed a considerable fuel consumption improvement of 18% when compared to the baseline diesel vehicle. The EPA 2027 GHG emission targets for Class 6-7 urban vocational vehicle can be achieved with a 48V P3 mild hybrid configuration when coupled with mandated engine improvements. The cost of ownership is lower for the 48V P3 mild hybrid architecture when compared to the baseline diesel vehicle. The full hybrid solutions for the P3 architecture had the highest cost of ownership mainly driven by the higher operating and maintenance costs.

Operation over the real-world drive cycle generated using GT-RealDrive demonstrated a lower delta in CO_2 reduction and freight ton efficiency improvements between the P3 48V mild hybrid and full hybrid solutions. It is critical to consider both certification and real-world drive cycles when optimizing the hybrid system specifications. Considering a two-year payback period, the final P3 350V hybrid powertrain solution for the Class 6-7 vocational vehicle provides a 33% freight ton efficiency improvement along with 27% reduction in CO_2 emissions, while a 48V mild hybrid system provides a 24% freight ton efficiency improvement along with 18% reduction in CO_2 emissions.

To further evaluate the potential of a 48V mild hybrid for heavy-duty applications, future studies will focus on evaluating the P3 mild hybrid architecture for Class 4-5 and Class 8 long-haul applications. Studies will also focus on evaluating the use of a 48V belt starter generator with a P3 mild hybrid architecture for Class 4-8 applications.

References

1. Rizzoni, G., Ahmed, Q., Arasu, M., and Oruganti, P.S., "Transformational Technologies Reshaping Transportation - An Academia Perspective," SAE Technical Paper 2019-01-2620, 2019, https://doi.org/10.4271/2019-01-2620.
2. Mock, P., "European Vehicle Market Statistics Pocketbook 2018/19 International Council on Clean Transportation Europe," https://theicct.org/sites/default/files/publications/ICCT_Pocketbook_2018_Final_20181205.pdf, accessed on Oct. 20, 2020.
3. Federal Register/Vol. 81, No. 206/Tuesday, October 25, 2016/ Rules and Regulations Greenhouse Gas Emissions and Fuel Efficiency Standards for Medium- and Heavy-Duty Engines and Vehicles—Phase 2.
4. EU, "Regulation (EU) 2019/1242 Setting CO2 Emission Performance Standards for New Heavy-Duty Vehicles," *Official Journal of the European Union*, July 25, 2019, L 198, 202.
5. Buysse, C. and Sharpe, B., "California's Advanced Clean Trucks Regulation: Sales Requirements for Zero-Emission Heavy-Duty Trucks, International Council on Clean Transportation," https://theicct.org/sites/default/files/publications/CA-HDV-EV-policy-update-jul212020.pdf, accessed on Oct. 20, 2020.
6. https://nacfe.org/emerging-technology/electric-trucks-2/viable-class-7-8/
7. https://www.ttnews.com/articles/nacfe-report-predicts-multiple-fuels-will-give-way-battery-electric
8. Roeth, M., "Transformational Technologies Reshaping Transportation - An Industry Perspective," SAE Technical Paper 2020-01-1945, 2020, https://doi.org/10.4271/2020-01-1945.
9. Greenhouse Gas Emissions and Fuel Efficiency Standards for Medium- and Heavy-Duty Engines and Vehicles - Phase 2, Regulatory Impact Analysis, EPA, NHTSA, EPA-420-R-16-900, August 2016
10. Minarcin, M., Rask, E., and Smith, M., "Challenges and Opportunities in Adoption of Hybrid Technologies in Medium and Heavy Duty Applications," SAE Technical Paper 2011-01-2251, 2011, https://doi.org/10.4271/2011-01-2251.
11. Gao, Z., Finney, C., Daw, C., LaClair, T. et al., "Comparative Study of Hybrid Powertrains on Fuel Saving, Emissions, and Component Energy Loss in HD Trucks," *SAE Int. J. Commer. Veh.* 7(2):414-431, 2014, doi:10.4271/2014-01-2326.
12. Proust, A. and Surcel, M., "Evaluation of Class 7 Diesel-Electric Hybrid Trucks," SAE Technical Paper 2012-01-1987, 2012, https://doi.org/10.4271/2012-01-1987
13. Yang, F., Xu, C., and Sun, J., "Design and Analysis of Parallel Hybrid Electric Vehicles for Heavy-Duty Truck Applications in a Total Cost of Ownership Framework," SAE Technical Paper 2018-01-5025, 2018, https://doi.org/10.4271/2018-01-5025.
14. Joshi, S., Dahodwala, M., Koehler, E., Franke, M. et al., "Trade-Off Analysis and Systematic Optimization of a Heavy-Duty Diesel Hybrid Powertrain," SAE Technical Paper 2020-01-0847, 2020, https://doi.org/10.4271/2020-01-0847.
15. Zhu, D., Pritchard, E.G.D., and Silverberg, L.M., "A New System Development Framework Driven by a Model-Based Testing Approach Bridged by Information Flow," *IEEE Systems Journal* 12(3):2917-2924, 2016.
16. A New Generation of Axial Flux EV Motors by: Kevin Clemens Electric & Hybrid Vehicle Technology Expo - Novi, MI, Automotive, Electronics & Test, Industrial Machinery, May 21, 2018
17. Joshi, S., Dahodwala, M., Koehler, E., Franke, M., Naber, J., et al., "Controls Development and Vehicle Drive Cycle Analysis of Integrated Turbocompounding, Electrification and Supercharging system," in *ASME, Proceedings of the Internal Combustion Engine Fall Technical Conference 2018*, CEF2018-9703
18. Ecker, M., Nieto, N., Käbitz, S., Schmalstieg, J. et al., "Calendar and Cycle Life Study of Li(NiMnCo)O2-Based 18650 Lithium-Ion Batteries," *Journal of Power Sources.*
19. Schmalstieg, J., Käbitz, S., Ecker, M., Sauer, D.U., "A Holistic Aging Model for Li(NiMnCo)O2 Based 18650 Lithium-Ion Batteries," *Journal of Power Sources*, 257, 2014, 325-334, ISSN 0378-7753, https://doi.org/10.1016/j.jpowsour.2014.02.012

20. Ehsani, M., Gao, Y., Emadi, A., *Modern Electric, Hybrid Electric, and Fuel Cell Vehicles: Fundamentals, Theory, and Design*, Second Edition (Power Electronics and Applications Series), 2009
21. California Air Resources Board, "Battery Cost for Heavy-Duty Electric Vehicles," Advanced Clean Transit, August 2016, https://ww3.arb.ca.gov/msprog/bus/battery_cost.pdf
22. Hunter, C. and Penev, M., "Market Segmentation Analysis of Medium and Heavy Duty Trucks with a Fuel Cell Emphasis," NREL, DOE Hydrogen and Fuel Cells Program, 2019, Annual Merit Review and Peer Evaluation Meeting, https://www.hydrogen.energy.gov/pdfs/review19/sa169_hunter_2019_o.pdf, accessed on Oct. 20, 2020
23. Austin, D., "Pricing Freight Transport to Account for External Costs," Working Paper Series Congressional Budget Office Washington, DC, March 2015, https://www.cbo.gov/sites/default/files/114th-congress-2015-2016/workingpaper/50049-Freight_Transport_Working_Paper-2.pdf, accessed on Oct. 20, 2020
24. United States Department of Transportation, "Average Freight Revenue per Ton-Mile," Bureau of Transportation Statistics, https://www.bts.gov/content/average-freight-revenue-ton-mile, accessed on Oct. 20, 2020
25. https://www.fev.com/en/what-we-do/software-and-testing-solutions/products/testing/calibration/topexpert-xcal.html
26. Smith, D., Graves, R., Lustbader, J., Kelly, K. et al., "Medium- and Heavy-Duty Vehicle Electrification, an Assessment of Technology and Knowledge Gaps," *ORNL, NREL, US Department of Energy, Office of Energy Efficiency & Renewable Energy*, Dec. 2019.

Contact Information

Mufaddel Dahodwala
Technical Specialist, Performance and Emissions
Commercial Engines; FEV North America, Inc.
dahodwala@fev.com

Koehler, Erik
Senior Department Manager, Performance and Emissions
Commercial Engines; FEV North America, Inc.
Koehler@fev.com

Acknowledgments

The authors would like to thank FEV North America, Inc. management for encouraging this research effort and providing the resources necessary to accomplish its goals. The authors would also like to thank those who took the time to review this paper and provided valuable feedback.

Definitions/Abbreviations

US - United States
GHG - Greenhouse Gas
EPA - Environmental Protection Agency
ARB - Air Resources Board
EU - European Union
CO_2 - Carbon Dioxide
OEM - Original Equipment Manufacturer
ZEV - Zero Emission Vehicle
NZEV - Near-Zero Emission Vehicle
NACFE - North American Council for Freight Efficiency
NMC - Nickel Manganese Cobalt Oxide Li Ion Battery
DC - Direct Current
BLDC - Brushless Direct Current
SOC - State of Charge
MPGe - Miles per Gallon Equivalent
BSFC - Brake Specific Fuel Consumption
FC - Fuel Consumption